Tracking Recharge and Groundwater Flow on Sonoma Mountain Using Geophysical Imaging

Lawrence M Thompson
B.S. Geology
Advisor: Robin Glas
Department of Geology
Sonoma State University
Rohnert Park Ca.

Senior Thesis
Spring 2020

Table of Contents

Abstract ……...3

Introduction …….3

a. Figure 1…….5

Methodology ……....7

a. Figure 2…….……8
b. Table 1……..……9

Interpretation and results…….10

a. Figure 3…….10
b. Figure 4……....11
c. Figure 5…….…..12
d. Figure 6……...13
e. Figure 7…….…..14

Discussion……15

a. Figure 8……16

Conclusion……...17

Reference…….19

Abstract

California's Coastal ranges are an integral source of riverine systems which are important to lotic ecosystems. These headwaters are becoming increasingly vulnerable as the climate changes the duration drought seasons in the region. Sonoma Mountain, located in the Northern Coastal Range, is the source of flow for the southernmost portion of the Russian River Watershed, which provides habitat for salmonid spawning and migration. Groundwater inputs to these headwater creeks are important for dry season flow, but the sources of recharge to these mountain aquifers have not been identified. We investigated the hydrogeologic function of a topographic ridge that runs parallel to a perennial spring that feeds a small stream located in the Fairfield Osborn Preserve on Sonoma Mountain. In order to determine the ridge's recharge potential, we conducted intersecting electrical resistivity tomography (ERT) lines at 1.0, 1.5, and 2 meter spacing coinciding with two boreholes that extends more than two meters in depth at the top of the ridge. Results indicate a shallow clay layer that acts as a barrier to groundwater that separates the spring from the ridge crest. Borehole data shows a clast supported formation of large, angular basalt fragments infilled with both sandy and silty loam. These results indicate that the ridge could potential be a feature of tectonic faulting. After analyzing the data, there is not a clear flow path feeding into the spring system from the pressure ridge. Future studies to further characterize this important spring in the Fairfield Osborne Nature Preserve include isotopic analysis of water age, and further geophysical imaging around the east and north of the spring system.

Introduction

Sources of water during the dry season are vital to California's Mediterranean Climate where ephemeral and intermittent streams make up 73% of the states stream network (Ode, Kincaid,

Fleming, and Rehn. 2011). With climate change extending span and intensity of dry seasons, lotic ecosystems reliant on rainfall are increasingly stressed as the wet seasons become more intense and the dry seasons elongate (Zhu, Jenkins, and Lund 2005). Species will undergo new stresses as the climate becomes more arid, so it will become increasingly important to understand and monitor perennial streams which maintain riparian growth year-round. The lack of perennial streams in the state of California increases the need for understanding groundwater resources that make up the base flow of the streams, which contributes to regional water resources in the dry season (Hershkovitz & Gasith, 2012).

The Northern Coastal Ranges of California are composed of the Franciscan Complex, an assemblage of marine sedimentary beds and metamorphic rocks accreted onto the North American Plate. This mélange is partially overlain by volcanics which have been uplifted and folded starting 150 million years ago. (Wakabayashi, 2015, Wagner, 2011). The Sonoma Volcanic complex reaches along the Costal Ranges adjacent to the Santa Rosa basin, Sonoma Valley, and Napa Valley creating Sonoma Mountain and the western portion of the Mayacama mountains (Wagner, 2011). It is composed of tuff, andesite, and basalt which has built Sonoma up to a height of 2463 ft, where it is affected by orographic cloud cover and precipitation during the dry season (Wagner, 2011, Smith & Barstad, 2004).

The Fairfield Osborne preserve covers 450 acres on the north east side of Sonoma Mountain near the summit. The preserve is comprised of grasslands and oak woodlands with some Douglas fir and chaparral covering the landscape. The headwaters of Copeland Creek originate in the preserve and are perennial in higher elevations but become intermittent as the creek flows down toward the adjacent floodplain (Smith & Barstad, 2004). The perennial headwaters of Copland Creek in Fairfield Osborne Preserve provide refuge for a fragile ecosystem that relies on constant

streamflow throughout the dry season from May through November (Miller, Bashford, and Strem, 2003).

The Geology of the Fairfield Osborne Preserve is composed entirely of basalt flows and rhyolitic ash (Mankinen, 1972). The Rodgers Creek fault zone strikes through Sonoma Mountain and the Fairfield Osborne Preserve. It is part of the Hayward fault zone and is currently active with the last major seismic event (>5.0M) occurring in 1969 (Hecker, 2005). The Rodgers creek fault zone is mostly composed of north east/southwest strike slip faults with some oblique-angled offshoots and pressure ridges. (Budding, Schwartz, & Oppenheimer, 1991).

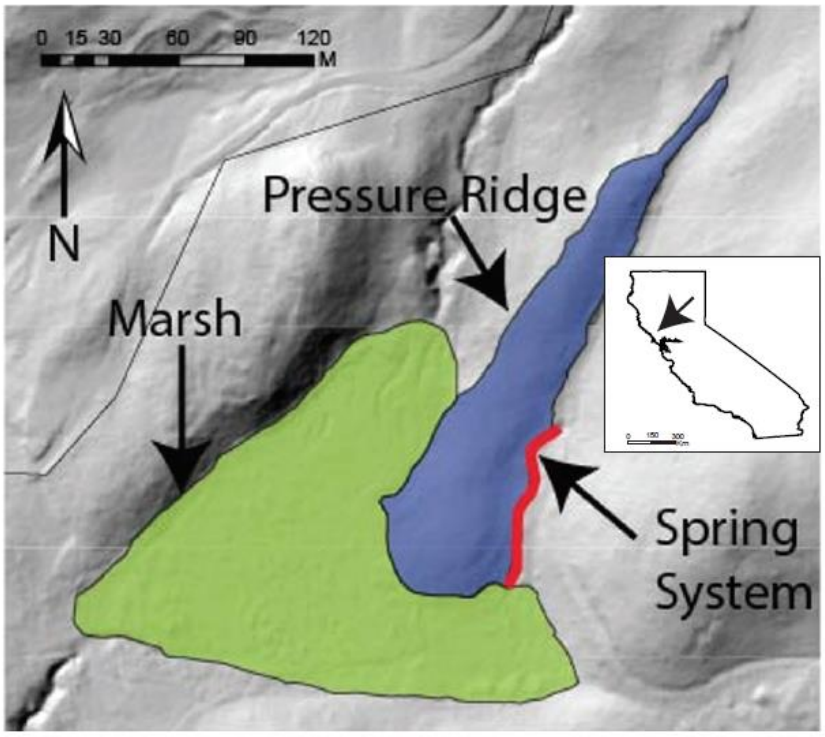

Figure 1: The study area is on the pressure ridge running down to the spring system. Showing the connectedness to the marsh highlights the impact of this spring fed stream on the local ecosystem.

Sonoma Mountain's soil is predominantly silty and clay loams with underlying clay deposits as a result from basalt weathering (USDA, 1972). Some gravitational slumps and alluvial deposits

can be found on the preserve while bank erosion is increasingly a problem in these headwaters, where the material is transported downstream toward the Laguna de Santa Rosa. Sediment buildup in the Laguna de Santa Rosa has been a problem which has caused numerous problems including the resurgence of non-native plants. (Potter and Hiatt 2020)

This study focuses on a ridge adjacent to a perennial spring on the Fairfield Osborne Preserve. The ridge is approximately three meters tall, 40 meters wide and 180 meters long. The spring is one of the only truly perennial sources of water on the preserve. It is the sole source for a stream which steadily gains in volume as it feeds into the marsh before joining Copeland creek (Figure 1). This year-round source of water is important for both Copeland creek and the surrounding ecosystem, however the subsurface structure and processes of the system have yet to be characterized. The adjacent ridge crest is relatively barren of trees and chaparral, and potential to be a zone of recharge for shallow groundwater which feeds the spring. The morphology of the ridge is likely a result of local fault geometry, which could act as a barrier or conduit for groundwater flow (Bense, Gleeson, Loveless, Bour, and Scibek, 2013).

To most effectively explore the structure of the subsurface and characterize the source and pathway of water to the spring, we used geophysical methods supported by bore hole data along the spring system and pressure ridge. The electrical resistivity tomography geophysical method was selected to investigate the shallow subsurface structure as it is sensitive to the lithological and hydrological properties that facilitate groundwater flow (Parsekian, Singha, Minsley, Holbrook and Slater, 2015). We used 2D Electrical Resistivity Tomography (ERT) to image the shallow sediment layers and couple these data with the borehole lithological logs to ground truth the geophysical data (Figure. 2). Our results make a significant contribution to the understanding

of dry season water sources in the Fairfield Osborn Preserve, and how subsurface pathways in this region are dependent upon tectonic fault structure.

Methodology

To characterize the groundwater flow around the pressure ridge we used geophysics and borehole data to predict the permeability of the subsurface. Using geoelectric methods (Electrical Resistivity Tomography, ERT) in tandem with boreholes allows for the non-unique geophysical models to be ground-truthed to real lithology, resulting in a more accurate map of the subsurface. The field analysis was conducted over a three-month period with work days in August and October 2019 with no period of precipitation in between the visits.

Electrical Resistivity Tomography lines were conducted using a multi-electrode system (SuperSting R1/IP). The array had 28 stainless steel electrodes what were evenly spaced out over the length of each line. We used a dipole-dipole array which has two sets of two electrodes. One set is injecting the current into the ground while the other set is receiving the current. It is standard that there is equal spacing distance for the current and receiving electrode pairs. When electricity is injected into the ground between electrodes a computer logs the voltage that is received and calculates the resistance between the pairs of electrodes.

Five ERT profiles were collected targeting the pressure ridge in the top five meters of the subsurface. Electrical geophysical methods were used because the can determine subsurface changes in saturation, porewater, groundwater conductivity, lithology, and clay content (Parsekian, Singha, Minsley, Holbrook and Slater, 2015). This method in non-unique in that multiple resistivity models can correspond to a single data set. The number of factors increases the ambiguity of the data so the addition of other methods such as borehole analysis are crucial to reduce error. Generally, more electrically conductive layers are clays, areas of saturation and

layers with smaller grain size, while less conductive materials include crystalline rock, cavities, and large rock fragments. (Samouëlian, Cousin, Tabbagh, Bruand, and Richard, 2005)

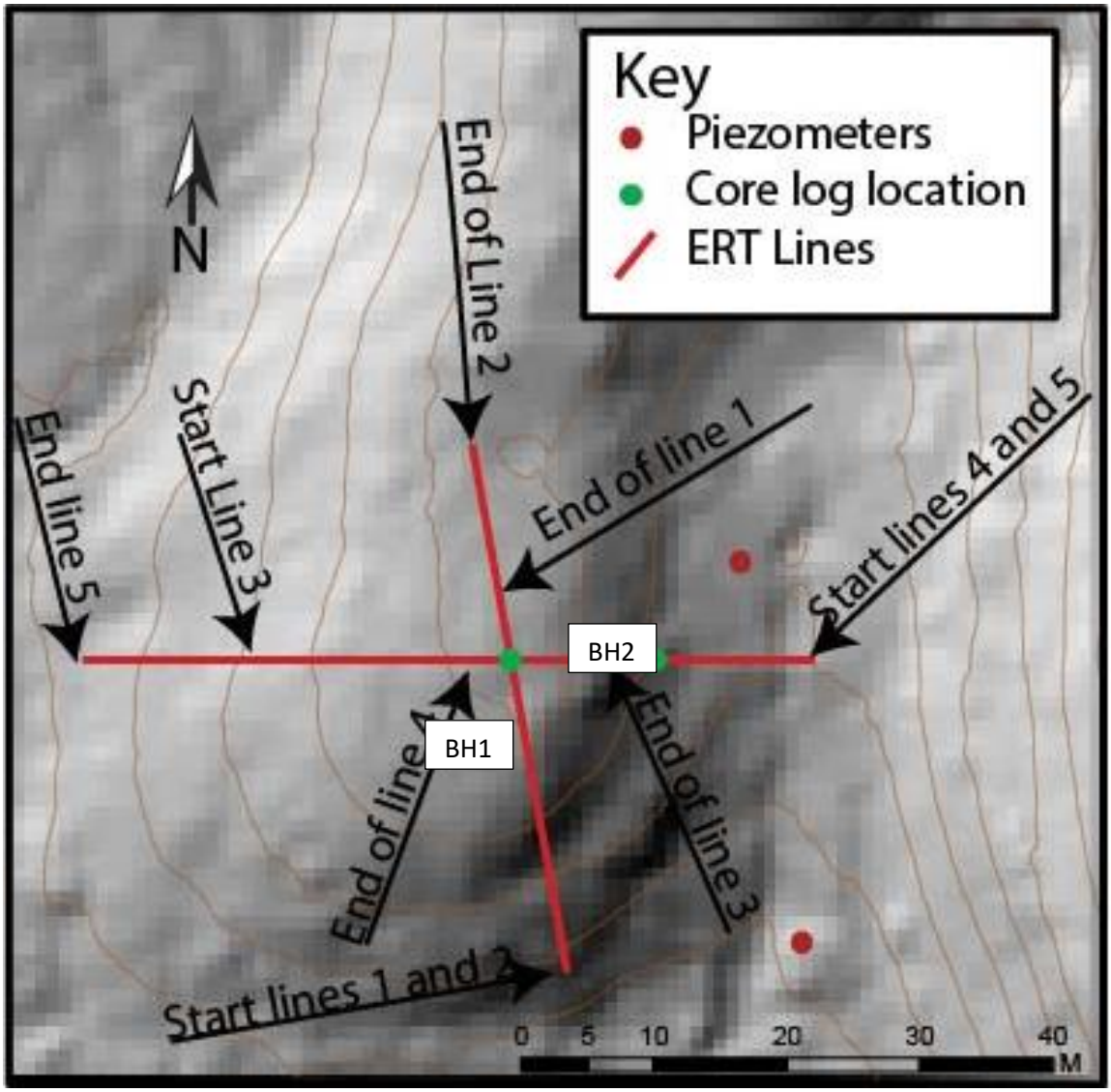

Figure 2 A DEM of the project area showing the locations of the geophysical lines. Two lines running south to north and three running east-west over the crest of the ridge. Additionally, the two boreholes are highlighted in green Borehole one (BH1) is at the intersection of the geophysical lines and borehole two (BH2) lies downslope to the east. There are also two piezometers in red which are next to the stream.

We instrumented this project with a SuperSting R1/IP system. For data collection we used 28 steel electrodes that were placed at 1m intervals for L1, L3, and L4. 1.5m for L2 and 2m spacing for L5. To reduce resistance-based error electrodes were watered to ensure that the contact resistance test was under 2000Ω. Using a portable Honda generator, we injected DC current into the ground with 1.2s signal pulse direction using a dipole-dipole electrode configuration in which the current source/receiver (A, B) and potential (M, N) electrode pairs are coupled adjacent to each other. The Dipole-Dipole array was advantageous for us because it prioritizes depth of investigation gathering more data points deeper in the ground. Each measurement was taken twice to check the accuracy of the reading, if the two measurements had a error difference of 2% or greater a third measurement was taken.

Apparent resistivity values were inverted using EarthImager 2D software (Advanced Geosciences, Inc.). The we used a smoothing multiplier of 10 to constrain the images. The smoothing function is used to get a broader image of subsurface using the specific data points gathered. I used a smoothing factor of 10 is the recommended setting for surface data (Advanced Geosciences, Inc. 2009). When considering model convergence criteria, we set the difference between the measured and calculated resistivity values to exhibit a root mean square error (RMS) of less than 5%.

Table 1

2D line	Survey Length	Receiver spacing	RMS (%)	L2
L1	27m	1m	8.39%	0.55
L2	40m	1.5m	5.09%	0.53
L3	27m	1m	3.76%	0.40
L4	27m	1m	6.86%	0.69
L5	54m	2m	3.22%	0.42

Using the average apparent resistivity of each line as a starting model all five Electrical tomography models converged within 5 iterations, both with normalized L2 values and the RMS being under 5% . Normalized L2 is the squared difference of the weighted errors between the synthetic and modeled data, normalized by the number of data points (Table 1).

Interpretation and Results

To ground truth the geophysical method and establish a core log of the study area, two boreholes were installed using a 41mm Shaw Backpack drill. Core samples were taken approximately every half meter when the drill bit was emptied of sediment (Figure 4). Our core log on the top of the pressure ridge (BH 1) show a thin layer of top soil leading into basalt cobbles and boulders between 15 to 38 cm in diameter in the top 2.4m. These rocks were angular and unweathered with some sandy loam infilling them. Drilling through this composition required large amounts of water due to the strain of the uneven surfaces of the rocks on the drill bit, and because the composition was permeable and continuously drained the water from the hole.

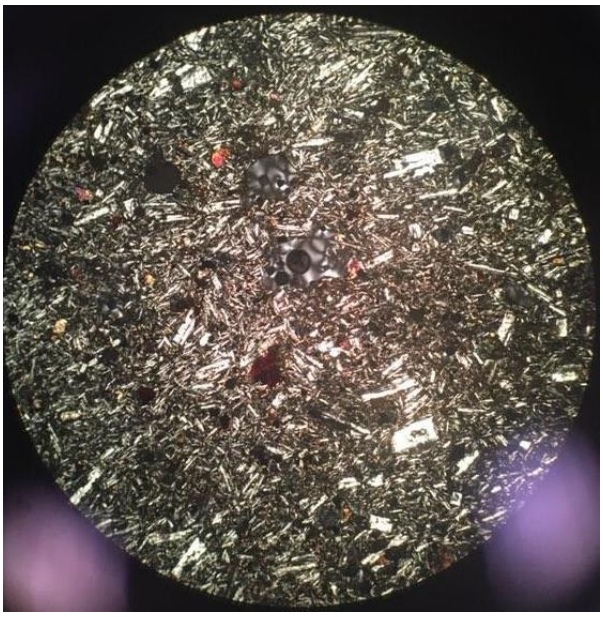

Figure 3 A thin section of the soft layer from 2.25-3.75m shown in cross-polarized light. It has an igneous origin and is probably Andesite or Basalt.

The cores extracted from BH 2 corresponded to a maximum depth of 3.7m. Shallow portions of BH2 were a sandy loam for the first three quarters of a meter from the surface. After this depth there is an abrupt transition into a dense clay.

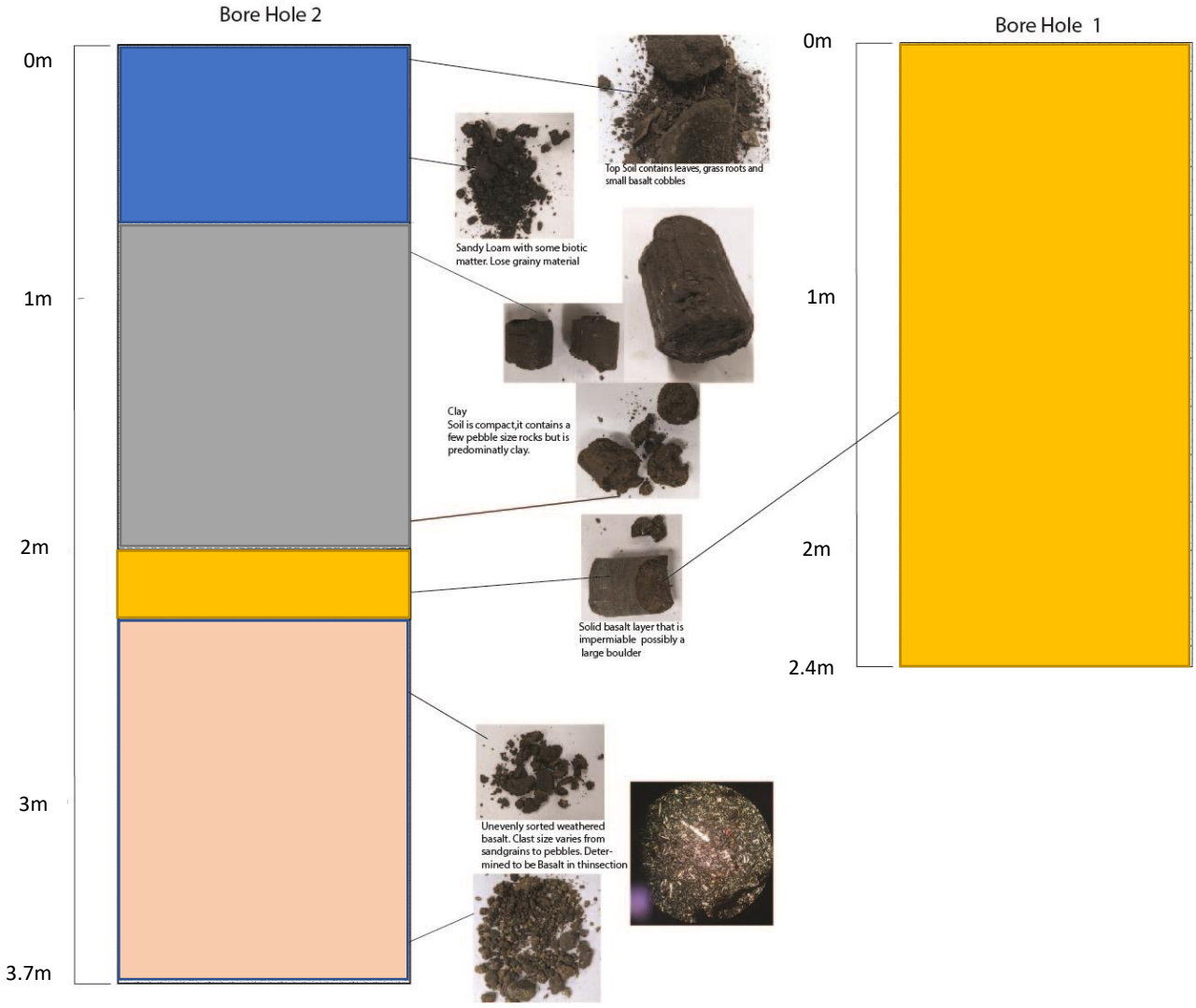

Figure 4 The sediment samples from borehole two showing the soil transition from the permeable surface to the highly conductive clay and finally into a weathered basalt layer.

The clay layer is from .75 m to 2m deep and was so compact that it retained its shape even after being pushed out of drill bit and transported to storage. Upon the termination of the dense clay, the drill bit hit a piece of basalt interface that when cored through resembled the same material as seen in BH 1. This basalt cobble is likely not a manifestation of competent bedrock as it gave way to a very soft layer of material at 2.25 m in depth that ranged in grain size from sand to pebbles. The sediment was examined in thin section and determined to be an andesite or a basalt that was severely weathered (Figure 3).

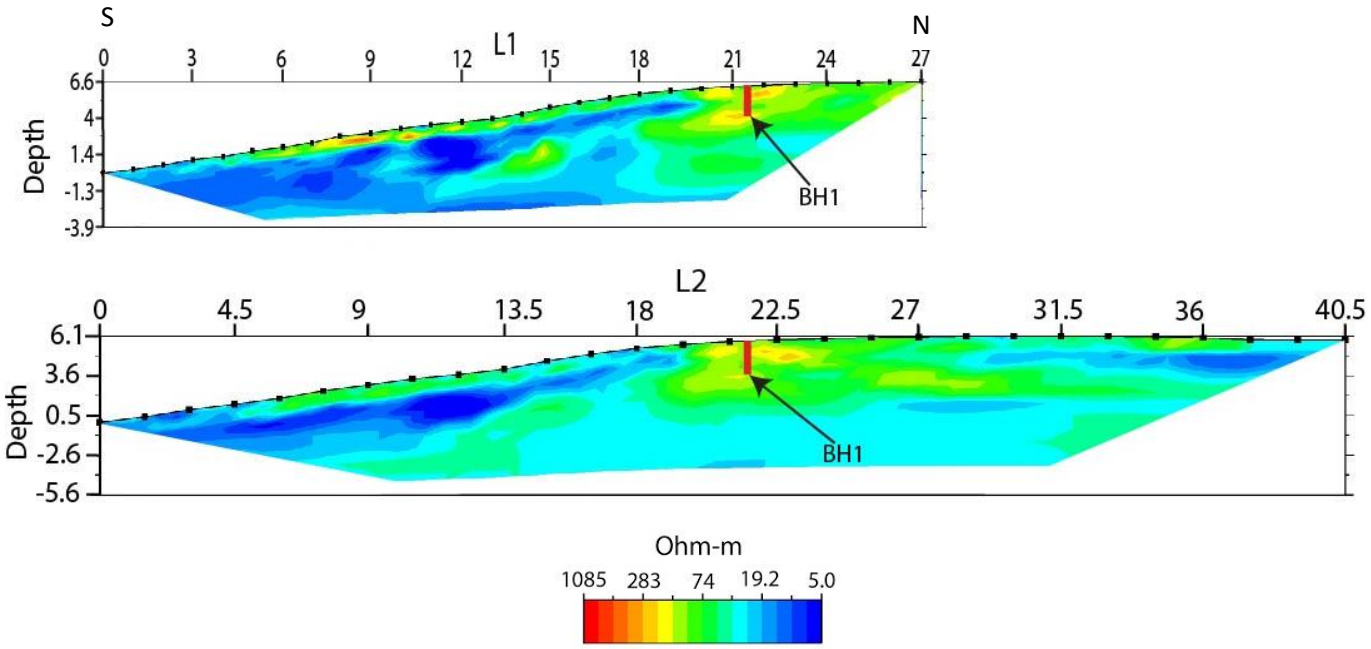

Figure 5 Tomograms (inverted resistivity images) of lines one (L1) and two (L2). These lines run south to north. Both show the location and depth of borehole one in the location it was drilled relative to the resistivity survey.

Due to the accessibility of the area the lines were taken over a three-month time period. The first three lines were completed in July 2019 and the last two in October 2019, and considering the lack of rainfall during this period we expected to observe an increase in the resistivity of the subsurface. The upper half meter of the subsurface did increase in resistivity as expected on lines L4-L5, under the assumption that there has been no structural changes in lithology or grain size.

Our north-south transect was composed of two lines (L1 and L2) with the same start point (Figure 5). L1 was 27 meters long while L2 was 39 meters to increase the depth of penetration, this was done to try to create an accurate image of the top three meters while also having a general idea of flow paths under the pressure ridge. The change in length allowed for different targets at depth and served to give more complete image of the subsurface.

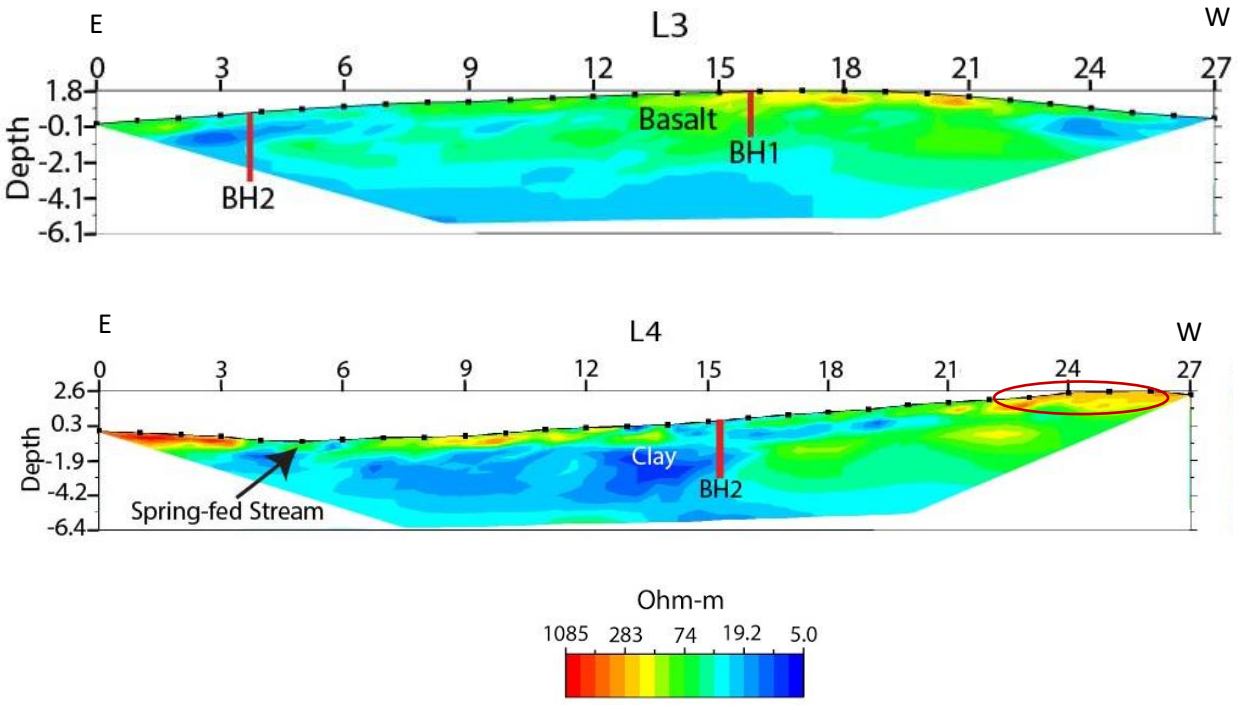

Figure 6 Tomograms of lines three and four from east to west. To scale depictions of the location and depth of boreholes are highlighted in red. The parts of the subsurface which were interpreted as clay and basalt have also been labeled as such. These images were taken two months apart, the difference in resistivity is due to the subsurface drying over summer (circled).

In L1 from the one-meter mark to the 19-meter mark there is a layer of low resistivity material that is approximately .5 meters deep. Between the 20-meter mark and the 24-meter mark there is a layer of high resistivity material that reaches down 3 meters. This was echoed in L2 with the addition of a high resistivity area between the 19- and 24-meter mark.

The east-west transect is composed of one long line that is split in the middle by L3 and L4 (Figure 6). Line (L5) runs across the whole pressure ridge while the two smaller lines (L3 and L4) overlap on the eastern side. L3 consists mostly of material with a resistivity of 70 Ohm-m and from the western edge to the 4-meter mark is a conductive feature of <10 ohm-m about one meter deep which corresponds to the borehole depth of clay. In L4 the These lines allow a more comprehensive image of the subsurface as there are shallow higher resolution surveys (0.5 m resolution) to compliment the deeper and more broad images (1.5 m resolution). Line L4 displays a conductive feature of <20 Ohm-m resistivity from 6 m to 16 m along the line, varying in depth from one to four meters.This feature also corresponds to clay encountered in L3 and BH2.

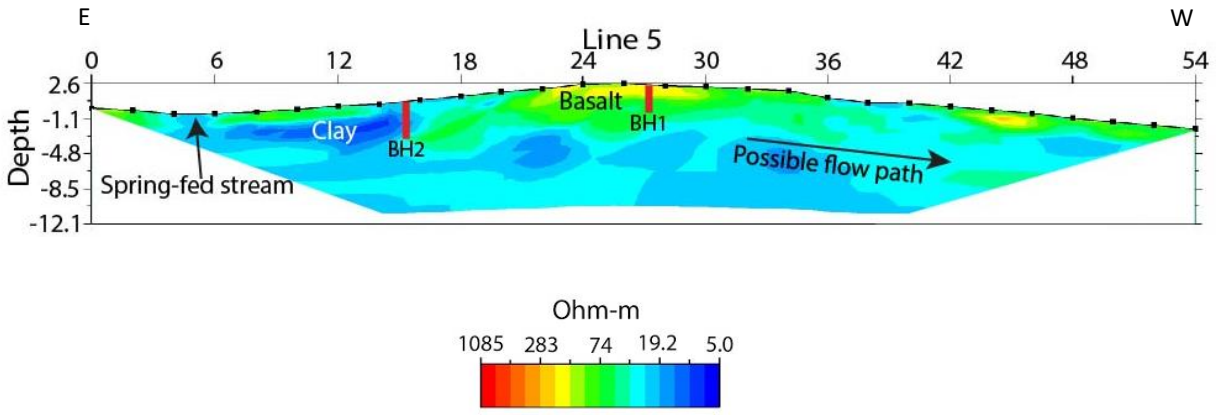

Figure 7 This tomogram (L5) shows the entire pressure ridge from east to west. This line was taken spacing the electrodes two meters apart which allowed for a wider and deeper image giving a more complete image of the pressure ridge.

L5 (figure 7) has two-meter spacing from the four-meter mark to the 16-meter mark is a layer of <20 ohm-m material that begins at a depth of one meter and continues down for two

before the increasing to >30 ohm-m. From the 17-meter mark to the 36-meter mark the resistivity is between 70-150 ohm-m in the first 4 meters in depth. Below the depth of approximately 4 m, the material ranges from 20 to 50 ohm-m.

The resistivity data were inverted using the AGI software EarthImager 2D, which utilizes a smooth model inversion. The smoothing factor of 10 that is generally used for surface surveys acts as a regularization constraint on the inverse model. The first step in this process consists of a starting model of average apparent resistivity imaged by the machine, which is then forward modeled to produce a synthetic dataset. This synthetic data set is then inverse modeled to a resistivity distribution of the subsurface. This process is repeated over and over, until the synthetic data set matches the field data set to a satisfactory degree. We imposed convergence criteria of 10% RMS such that the iterative process converges upon a 10% error or less between modeled and field data. Before modeling the data, we removed 12-15% of the data, using the data misfit histogram. This was to reduce the L2 and RMS in a uniform and reproducible manner. All of the models converged within five iterations of the program (Table 1). All of the lines were given the same color map ranging from 5 to 1085 Ohm meters.

Discussion

Bedrock in this area is made up of basalt which, when intact and unweathered would be expected to exhibit higher resistivities (>3000 Ωm), however the depth to competent bedrock in this area is still unknown because the low resistivity at the bottom of our images is not what would be expected in bedrock. Due to difficulty drilling our core logs were only a few meters deep and we never reached a solid layer of basalt although there were some large clasts of basalt in the upper most portion of the ridge, as well as the deeper portion of BH2 (between 2.5-4 meters) was

pulverized basalt that had undergone both physical and chemical weathering. The confined layer was pulverized igneous rock most likely basalt or andesite the same as our assumed bedrock. Tectonic events in the formation of the pressure ridge could have pulverized in the bedrock, lowering the depth to competent bedrock in the area.

Our results also suggest that the groundwater feeding this spring follows a path along the fault system. Bense and others (2013) have indicated that tectonic faulting can either facilitate or inhibit groundwater flow, depending on the nature of the fault and the materials surrounding it. In this case, we believe that groundwater flow is facilitated by the fault itself, which runs parallel in strike to the pressure ridge. The material surrounding the fault seems to be clay rich and relatively impermeable, suggesting that the weathered basalt has been further pulverized by the pressure of the ridge and fault. Future seismic events and fault activity of the Rodger's Creek fault system within the Fairfield Osborn Preserve will therefore have an effect on this unique water source, and future work could monitor seismic activity and correlate it to volumetric increases or decreases in spring discharge.

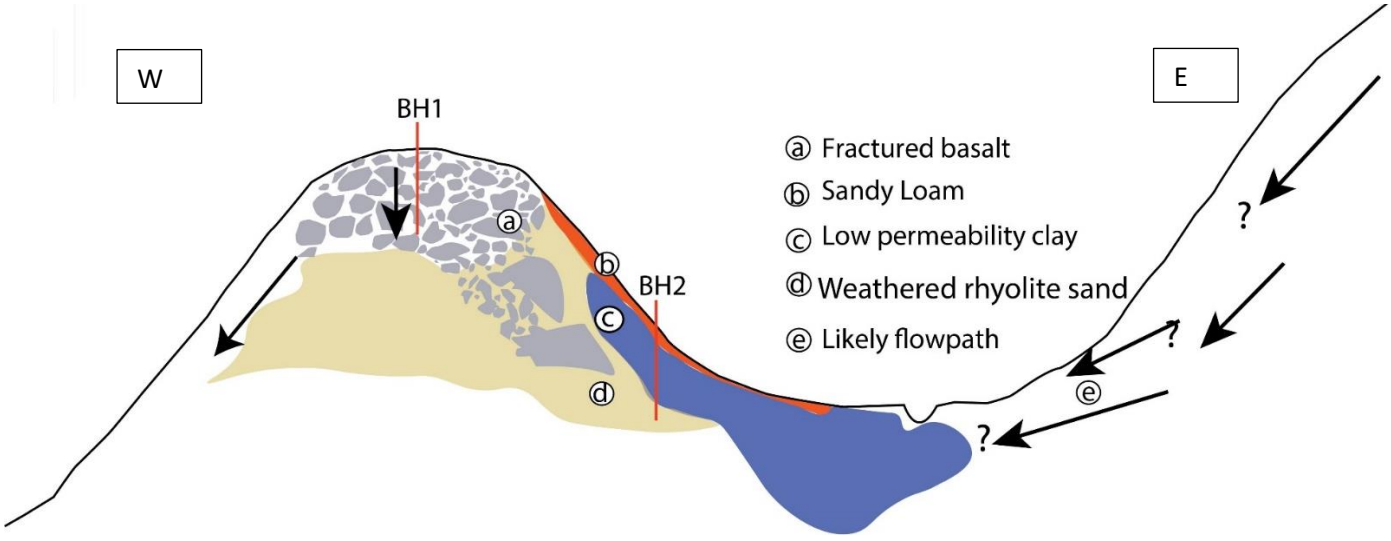

Figure 8 A conceptual model of the groundwater flow in and around the pressure ridge

Our work indicates there is a thick layer of impermeable clay around the spring system, likely formed from a combination of weathering and tectonic activity. Resistivity observations indicated the presence of a low resistance (appx. 5 Ωm) material starting at roughly a meter depth. Clay is associated with the erosion of the Sonoma Mountain Volcanics which are silicate-rich and exposed to water. Dense impermeable layers often act as a confining layer for aquifers, and our results suggest that the clay is acting as both confining layer and an impermeable boundary for recharge at the ridge crest.

The results of our geophysical models integrated with the borehole data were use to created a conceptual model of preferential flow paths in the pressure ridge (Figure 8). Our model supports the interpretation the precipitation infiltrates in the crest of the pressure ridge but the precipitated water does not drain down toward the spring system to the east as originally hypothesized, because low permeability clay layer likely impedes flow. Instead, water that is infiltrated at the crest of the ridge is likely directly into the marsh to the west by way of higher resistivity layer that is interpreted to have a higher sand and cobble content. The propagation of water throughout the spring system and feeding the small stream is therefore driven by downgradient flow of groundwater originating along the strike of the ridge. This water is then forced up to the surface as it reaches the clay that lies below and alongside the ridge. The model assumes there is a hydrologically confined layer running down the hill and abutting the pressure ridge which contains a break in the confining layer allowing the spring to form.

Conclusion

Electrical Resistivity Tomography was gathered and interpreted with overlapping borehole data to better understand the source of a spring located in the Fairfield Osborne Nature Preserve.

Results suggest that the top of the adjacent pressure ridge is a recharge zone toward a marsh to the west of the ridge, because there is no clear hydrologic connection between the spring and top of the pressure ridge. The ridge and spring are separated by an impermeable clay layer caused by the weathering of basalt bedrock that was likely pulverized in the formation of the tectonic pressure ridge. Therefore, the source of groundwater feeding this spring likely comes from higher elevations to the north and flows along the fault system, being pushed to the surface by impermeable clay material.

It is possible that some of the water feeding this spring system comes from the eastern side of the spring, and further investigations should be carried out to characterize this source of groundwater flow. Clarification of this would be beneficial to more accurately understand the constraints of the spring system under the pressure of climate change. groundwater. As dry seasons lengthen and intensify, there will be changes to precipitation amounts that recharge this system during the wet season. Age dating the spring water using isotopic techniques could elucidate the transit time of water to the spring, so that as the local climate warms and inputs to the water cycle change, we can better predict the longevity of the spring and its surrounding lotic ecosystem. Furthermore, our work has shown that this important water source for the preserve is heavily dependent upon tectonic structures in the subsurface; namely, a north-south striking fault as well as pulverized material that has been formed by this pressure ridge. This indicates that any future tectonic activity may divert, open, or even close this spring. We suggest careful monitoring of the spring discharge in conjunction with seismic monitoring to determine which of these cases is most likely to occur. Hydrologic and geologic monitoring of the spring will allow the preserve to better characterize its water sources, as well as predict changes to its hydrology in the face of climatic and geologic changes in the region.

Citations

Bense, V. F., Gleeson, T., Loveless, S. E., Bour, O., & Scibek, J. (2013). Fault zone hydrogeology. *Earth-Science Reviews, 127, 171–192.*

Budding, K. E., Schwartz, D. P., & Oppenheimer, D. H. (1991). Slip rate, earthquake recurrence, and seismogenic potential of the Rodgers Creek Fault Zone, northern California: Initial results. *Geophysical Research Letters, 18(3), 447–450.* doi:10.1029/91gl00465

Grantham, T. E., Merenlender, A. M., & Resh, V. H. (2010). Climatic influences and anthropogenic stressors: an integrated framework for streamflow management in Mediterranean-climate California, U.S.A. *Freshwater Biology, 55, 188–204.* doi:10.1111/j.1365-2427.2009.02379.x

Gasith, A. and Resh, V. H., Streams in Mediterranean climate regions: Abiotic influences and biotic responses to predictable seasonal events. *Annual Review of Ecology and systematics*. Vol. 30:51-81 (Volume publication date 1999) DOI;10.1146/annurev.ecosys.30.1.51

Hershkovitz, Y., & Gasith, A. (2012). Resistance, resilience, and community dynamics in mediterranean-climate streams. *Hydrobiologia, 719(1), 59–75.* doi:10.1007/s10750-012-1387-3

Wakabayashi, J. (2015). Anatomy of a subduction complex: architecture of the Franciscan Complex, California, at multiple length and time scales. *International Geology Review*, 57(5-8), 669–746. doi:10.1080/00206814.2014.998728

Mankinen, E. A. (1972). Paleomagnetism and Potassium-Argon Ages of the Sonoma Volcanics, California. *Geological Society of America Bulletin, 83(7), 2063.* doi:10.1130/0016-7606(1972)83[2063:papaot]2.0.co;2

Parsekian, A. D., Singha, K., Minsley, B. J., Holbrook, W. S., & Slater, L. (2015). Multiscale geophysical imaging of the critical zone. *Reviews of Geophysics, 53(1), 1–26.* doi:10.1002/2014rg000465

Potter, C., & Hiatt, S. (2009). Modeling river flows and sediment dynamics for the Laguna de Santa Rosa watershed in Northern California. *Journal of soil and water conservation*, *64*(6), 383-393.

Samouëlian, A., Cousin, I., Tabbagh, A., Bruand, A., & Richard, G. (2005). Electrical resistivity survey in soil science: a review. *Soil and Tillage research*, *83*(2), 173-193.

United States Department of Agriculture. Forest service and Soil Conservation Service. May 1972. *Soil Survey*: Sonoma County, California.

Zhu, T., Jenkins M. W., Lund J.R. (2005) Estimated Impacts of Climate Warming on California Water Availability Under Twelve Future Climate Scenarios. *Journal of the American Water Resources Association.* 1027-1038

Zonge, Ken, Jeff Wynn, and Scott Urquhart. "Resistivity, induced polarization, and complex resistivity." In *Near-surface geophysics*, pp. 265-300. Society of Exploration Geophysicists, 2005.